IIETA International Information and Engineering Technology Association
Advancing the World of Information and Engineering

Journal Européen des Systèmes Automatisés
Vol. 58, No. 11, November, 2025, pp. 2427-2433
Journal homepage: http://iieta.org/journals/jesa

The BLDC Motor Design for Current Industrial and Civil Applications

Phan Hoai Nam, Tran Đuc Chuyen*

Faculty of Electrical Engineering-Automation, University of Economics-Technology for Industries, Hanoi 10000, Vietnam

Corresponding Author Email: tdchuyen@uneti.edu.vn

https://doi.org/10.18280/jesa.581119

Received: 13 October 2025
Revised: 15 November 2025
Accepted: 21 November 2025
Available online: 30 November 2025

Keywords:
motor design, brushless DC motor, ANSYS Maxwell, finite element simulation, permanent magnet, industrial machines, civilian machines

ABSTRACT

Nowadays, the importance of industrial and civil applications such as washing machines, air conditioners, pump fans, exhaust fans, electric vehicles, etc., the application of brushless DC motors (BLDC) is becoming more and more urgent due to the high demand for efficiency, energy saving and wide applicability in many fields such as drones, household appliances and industrial machines. Currently, many researchers in the world have focused on designing and optimizing BLDC motors to improve efficiency, reliability and reduce production costs. This study aims to design and simulate a small capacity BLDC motor (320 W, 12 V) using high-performance NdFeB magnets, through ANSYS Maxwell simulation software. The research results contribute to providing optimal technical parameters and specific design models, meeting practical requirements such as stable power, high efficiency and minimizing energy loss, helping to orientate wider application in industry and civil use for this type of electric motor in Vietnam.

1. INTRODUCTION

The BLDC electric motor is a type of synchronous rotating electric machine that uses permanent magnets on the rotor and a control system using power electronic valves instead of carbon brushes and commutators of traditional DC motors (which are often damaged). By eliminating friction and losses due to carbon brushes, BLDC motors have many advantages such as high efficiency, large starting torque, high power density and torque per weight, smooth operation and high reliability [1-5]. With these advantages, BLDC is now widely used in civil and industrial electrical equipment such as CNC (Computer Numerical Control) mechanical processing machines, drilling machines, lathes, cutting machines, conveyor motors, joints of industrial robot arms, etc. [6-9]. Especially in electric vehicles such as electric vehicles, electric bicycles, electric cars, devices that require high performance and durability, ensuring economy as well as good (precise) control of torque and current [10-15]. The need to develop high-performance BLDC electric motors in industry and civil use is becoming increasingly urgent in the context of air pollution, energy saving and using clean energy to protect the environment, [2, 4, 5, 16-20].

When analyzing with some other motors, we see the following differences:

•Asynchronous motor (IM): has low cost and durability but is limited in applications that require speed control, has low efficiency [21-23].

•Switched reluctance motor (SRM) has outstanding durability but is strongly limited by noise, vibration and complex control system [24, 25].

•Synchronous motors (PMSM/IPM) are the most optimal in terms of performance but have high costs, require complex control equipment, and are often used in industry and in mechanical processing machines.

From these limitations, BLDC motors are the best balanced choice for the above applications with the advantages of high efficiency (85-96%), large starting torque, compact size, light weight, fast and accurate response, low maintenance due to no carbon brushes, smooth and quiet operation, common manufacturing materials suitable for mass production, [7-9, 20-22]. In addition, in the country, currently, research on simulation, control, and design of BLDC motors has not received much attention, [10, 11]. These studies have not yet focused on the use of specialized design software such as Ansys Maxwell with high accuracy close to reality.

2. DESIGN RESEARCH CONTENT

2.1 Theoretical basis for design research

BLDC motors are gradually replacing brushed motors in most consumer and industrial electronics: hard drives, fan drives, model aircraft, hand tools, industrial robots, Computer Numerical Control (CNC) metalworking machinery equipment, washing machines, industrial pumps/fans, personal vehicles such as electric vehicles, industrial robots, medical devices, smart home appliances (home washing machines), refrigeration compressors, HVAC (Heating, ventilation and air conditioning systems), etc.

In the industry, BLDC is ideal for motion control, industrial robots, CNC machine tools, thanks to the ability to control torque precisely, directly control torque during the control process, BLDC motors operate with a wide speed range and low maintenance and maintenance costs.

BLDC motors are designed with an internal rotor as shown in Figure 1, this type of structure is also called "Inrunner". With this design, the permanent magnets are located above the rotor inside, and this rotor rotates inside the stator coils. Besides, there is also another popular configuration called "outrunner", where the stator coil is located in the center and the rotor with permanent magnets rotates around the outside. With this type of structure, it is often used in Hub motors of electric vehicles, industrial and civil machine motors.

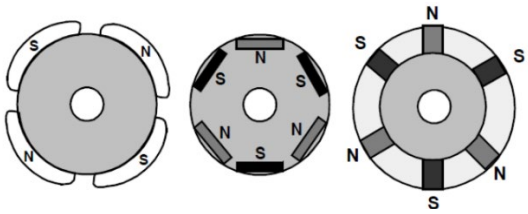

Figure 1. Some types of BLDC motor structures

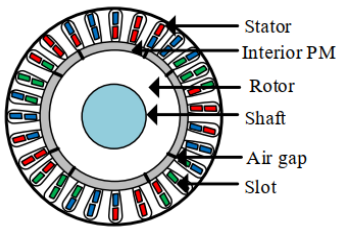

(a) BLDC motor has rotor inside

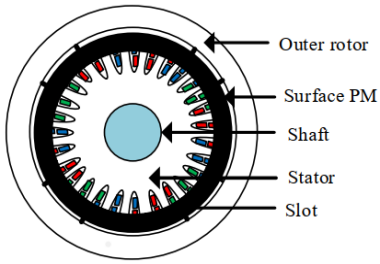

(b) BLDC motor has rotor on the outside

Figure 2. Two types of BLDC motors are currently being researched

In the field of industrial machinery, brushless motors are preferred because of their ability to accurately control speed and position, and their ability to adjust torque much better than other motors. In Figure 2, both types of BLDC motors are being researched, designed, and manufactured for application.

From there, the authors researched the BLDC design as shown in Figure 3.

Figure 3. External rotor BLDC motor

Research on BLDC motors for industrial and civil use is an important and rapidly developing field: optimizing stator and rotor structures to reduce weight and size while still ensuring performance.

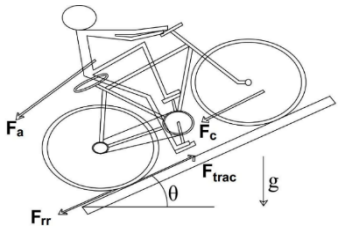

Figure 4. An example of the total force acting on a vehicle is the application of BLDC for electric bicycles

Select high quality materials for coils (copper, aluminum), permanent magnets (Neodymium - NdFeB) and laminated steel cores to reduce energy loss and increase efficiency. Control problem with trapezoidal electromotive force to optimize torque, reduce noise and increase energy efficiency, used for industrial machines, civil electric vehicles (see Figure 4).

For example, Figure 4 shows the forces acting on a vehicle when moving on a slope where Fa is the aerodynamic drag force, Frr the rolling resistance, Fc the climbing force, Ftrac the total drag force, g the acceleration of gravity, θ the slope angle. The reference vehicle is a two-wheeled vehicle with the parameters as shown in Table 1 below.

Table 1. The main parameters of BLDC

Symbol	Parameters	Values	Unit
m	Total mass	250	kg
g	Acceleration of gravity	9.81	m/s^2
μ_{rr}	Rolling resistance coefficient	0.004	-
r_{wheel}	Wheel radius	0.1125	m
δ	Air density	1.23	kg/m^2
C_d	Air drag coefficient	0.88	-
v	Speed	19.1	km/h
θ	Slope	0	Degree

In today's industry, machines also need precise control, aiming for high quality work (Figure 5).

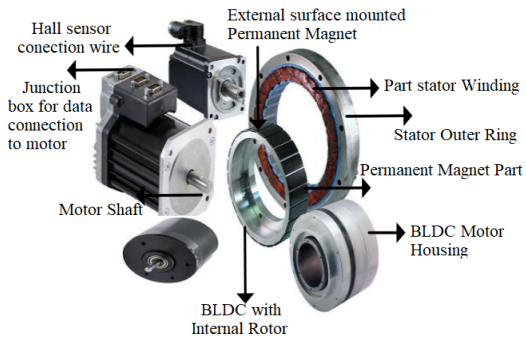

Figure 5. The BLDC motors used in industrial machinery and civil

BLDC are being widely used in electronic devices such as fans, computers, printers, hand-held cutting machines, air-conditioning fans, car air-conditioning fans, drones, as well as in the automation and robotics industry.

2.2 The BLDC motor design calculation in industrial and civil fields

The BLDC calculation research process is a complex process that includes many steps, from determining technical

requirements to simulation and actual testing:

Rated torque is expressed through power Po and angular speed ω [3]:

$$T = \frac{P_o}{\omega} \quad (1)$$

The following formulas are referenced by the author in document [4]. Mechanical angular velocity:

$$\vartheta_m = \frac{T}{\omega} \quad (2)$$

Synchronous angular velocity of the motor:

$$\vartheta_e = \frac{N_m}{2}.w_m \quad (3)$$

In which, N_m is the number of magnetic poles.

Basic electrical frequency:

$$f_e = \frac{\vartheta_e}{2.\pi} \quad (4)$$

Number of stator slots:

$$N_s = N_{sp}.N_{ph} \quad (5)$$

In which, the component $N_{sp} = \frac{N_s}{N_{ph}} \geq N_m$ is the number of slots per phase. Number of phases $N_{ph} = 3$.

Number of slots per phase under one pole:

$$N_{spp} = \frac{N_{sp}}{N_m} \quad (6)$$

where, N_m is the number of poles of the electromagnet.

The number of slots per pole is counted:

$$N_{sm} = N_{spp}.N_{ph} \quad (7)$$

Step coefficient:

$$\alpha_{cp} = \frac{int(N_{sm})}{N_{sm}} = \frac{\tau_c}{\tau_p} \quad (8)$$

Extreme step angle:

$$\theta_p = \frac{2.\pi}{N_m} \quad (9)$$

Groove step angle:

$$\theta_s = \frac{2.\pi}{N_s} \quad (10)$$

Electric angle, groove step:

$$\theta_{se} = \frac{\pi}{N_{sm}} \quad (11)$$

Stator pole step:

$$\tau_p = R_{os}.\theta_p \quad (12)$$

Winding step:

$$\tau_c = \alpha_{cp}.\tau_p \quad (13)$$

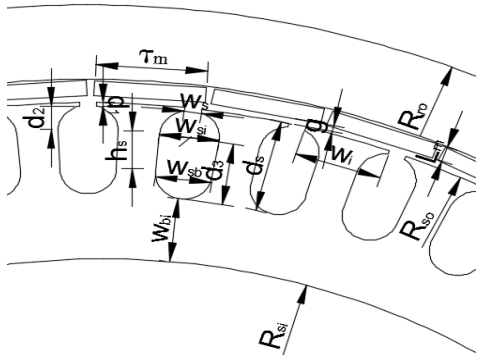

Figure 6. Detailed dimensions of a part of the engine

Figure 6 shows the dimensions of the BLDC motor with d_1 being the height of the groove neck, w_{si}, w_{sb} components, upper and lower body width, h_s being the height of the groove, etc. Below is how to determine the dimensions of the BLDC motor studied in this study:

$$d_2 = \frac{w_{si}}{2} \quad (14)$$

$$d_3 = \frac{w_{sb}}{2} + h_s \quad (15)$$

$$w_t = \tau_c - w_s \quad (16)$$

Inner radius of stator:

$$R_{si} = R_{so} - d_s - w_{bi} \quad (17)$$

In which, d_s is the outer radius of the rotor:

$$d_s = d_1 + d_2 + d_3 \quad (18)$$

The inner radius of the rotor R_{ri} is:

$$R_{ri} = R_{so} + L_m + g \quad (19)$$

where, $g = \left(0{,}1 + 0{,}012.\sqrt[3]{P_o}\right).10^{-3}$ [24].

Distribution coefficient:

$$k_{d1} = \frac{sin\left(\frac{N_{spp}.\theta_{se}}{2}\right)}{N_{spp}.sin\left(\frac{\theta_{se}}{2}\right)} \quad (20)$$

Step coefficient:

$$k_p = \alpha_{cp} \quad (21)$$

Slope coefficient:

$$k_s = 1 - \frac{\theta_{se}}{2.\pi} \quad (22)$$

Flux concentration coefficient:

$$C_\phi = \frac{2.\alpha_m}{1+\alpha_m} \quad (23)$$

where, $\alpha_m = \frac{\tau_m}{\tau_p}$ fractional magnet coefficient, τ_m is the width of the magnet

Environmental constant:

$$P_c = \frac{l_m}{g.C_\phi} \quad (24)$$

With, l_m is the length of the magnet.

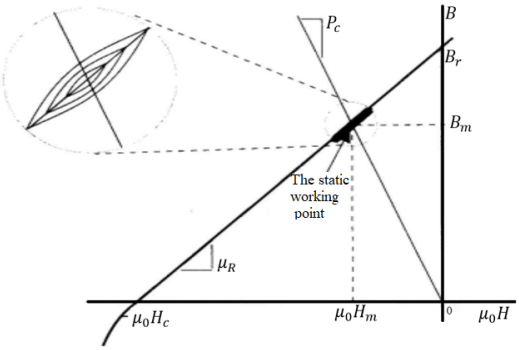

Figure 7. Demagnetization curve of permanent magnet

In Figure 7, the B axis is the magnetic flux density value in the steel core, and the $\mu_o H$ axis is the magnetic flux density value in the air, with the values B_r is the remanent magnetism, B_m the maximum magnetic flux value, μ_r μ_o the permeability of the steel core and the permeability of the air, H_c is the coercive force, H_m the maximum magnetic field strength.

$$A_g = \frac{\tau_p.L.(1+\alpha_m)}{2} \quad (25)$$

Initial air gap flux density:

$$B_g = \frac{C_\phi}{1+\frac{\mu_R.k_c.k_{ml}}{P_c}}.B_r \quad (26)$$

In which, B_r is the residual magnetic density.

The air gap flux:

$$\phi_g = B_g.A_g \quad (27)$$

Preliminary yoke width:

$$\omega_{bi} = \frac{\phi_g}{2.B_{max}.k_{st}.L} \quad (28)$$

Compression coefficient K_{st} = 0.95. B_{max} component of allowable magnetic flux density in the yoke B_{max} = 1.45 T.

Preliminary tooth width:

$$\omega_{tb} = \frac{2}{N_{sm}}.w_{bi} \quad (29)$$

Cross section of the slot containing the preliminary winding:

$$A_s = h_s.\left[\theta_s.\left(R_{so} - d_1 - \frac{h_s}{2} - d_2\right) - w_{tb}\right] + \pi.\frac{w_{sb}^2}{4} \quad (30)$$

Maximum counter-electromotive force:

$$e_{max} = N_m.k_d.k_p.k_s.B_g.L.R_{ro}.N_{spp}.n_s.w_m \quad (31)$$

Peak groove current:

$$I_s = \frac{T.w_m}{e_{max}} \quad (32)$$

Primary phase current:

$$I_{ph} = \frac{I_s}{N_{ph}.\sqrt{\frac{3}{2}}} \quad (33)$$

Peak winding current density:

$$J_c = \frac{I_s}{k_{cp}.A_s} \quad (34)$$

Number of fibers in 1 slot:

$$u_r = \frac{1000000.4.A_s}{\pi.d.d.n_s} \quad (35)$$

From the above analytical calculation expressions, we conduct simulation research to get the results in part three as follows.

Sundaram et al. [23] confirmed that the 51-slot/46-pole combination is the optimal configuration for in-wheel PMSM hub motors in two-wheeler electric vehicles due to its low cogging torque, reduced core losses, and superior overall performance

The mesh was generated with a total of 210,750 elements. The simulation was configured in transient mode over a time interval from 0 to 0.02 s with a fixed time step of 0.002 s. ANSYS Maxwell 3D was used for the electromagnetic analysis, and after the simulation was completed, the corresponding results were obtained.

3. RESEARCH RESULTS AND DISCUSSION

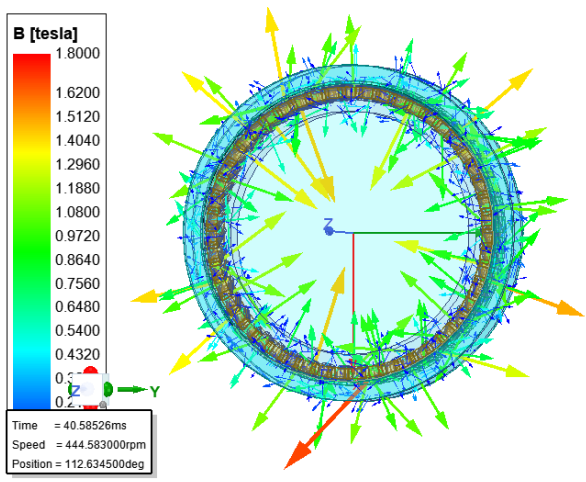

Figure 8. Flux density of BLDC motor

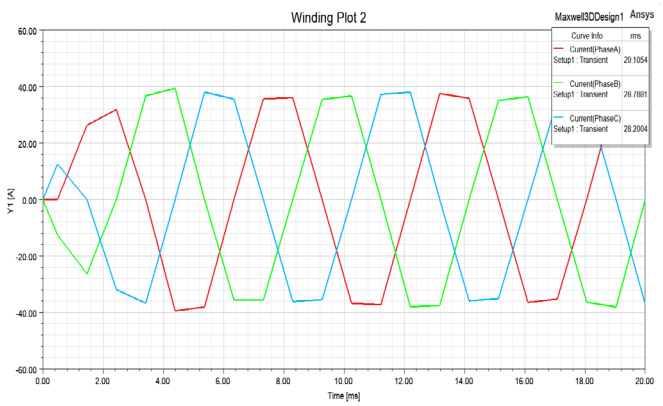

Figure 9. BLDC motor stator current

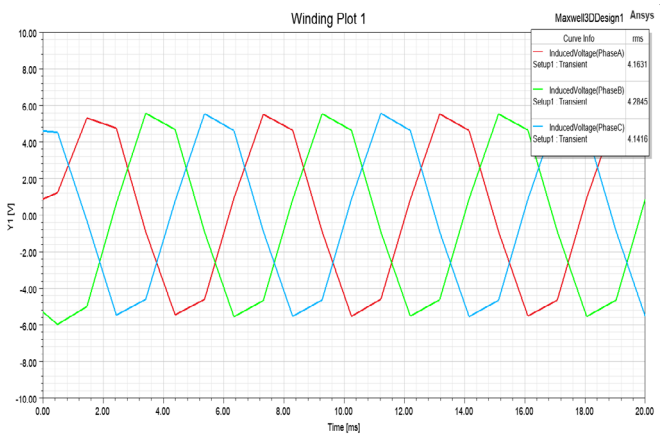

Figure 10. BLDC motor stator voltage

The application of generator calculation and design methods, especially the finite element method (FEM), has proven to be highly reliable in simulating electric motors. Ansys Maxwell software is a dedicated tool for simulating electric machines, using finite element analysis techniques based on Maxwell's equations to evaluate and analyze the electromagnetic characteristics of the device.

Faraday's law of induction: $\nabla \times E = -\frac{\partial B}{\partial t}$

Gauss's law of magnetic field: $\nabla \bullet B = 0$

Ampere's law: $\nabla \times H = J + \frac{\partial D}{\partial t}$

According to Gauss's law of electric field: $\nabla \bullet D = \rho$

We have the following simulation results:

Looking at the simulation results of Figure 8, we see: magnetic flux density is a key factor, directly affecting the performance, always creating inertial torque (during the control and working process - ensuring torque), optimization in the working process achieves high quality during the operation of the motor.

From Figure 9 and Figure 10, we have the transmitted power calculated:

$$S_{output} = 3*Sa = 3*4.1*28 = 344.4\ W \quad (36)$$

$$P_{output} = S_{output}.\cos\varphi = 373.86\ *1 = 344.4\ W \quad (37)$$

From Figure 9, the shaft power is:

$$P_{shaft} = \frac{T * n}{9.55} = \frac{6.39 \times 445}{9.55} \approx 312\ W \quad (38)$$

In which, component n is the engine rotation speed. From Eqs. (37) and (38), we have the engine efficiency:

$$\eta = \frac{P_{truc}}{P_{phát}} = \frac{312}{344.4} \approx 91\% \quad (39)$$

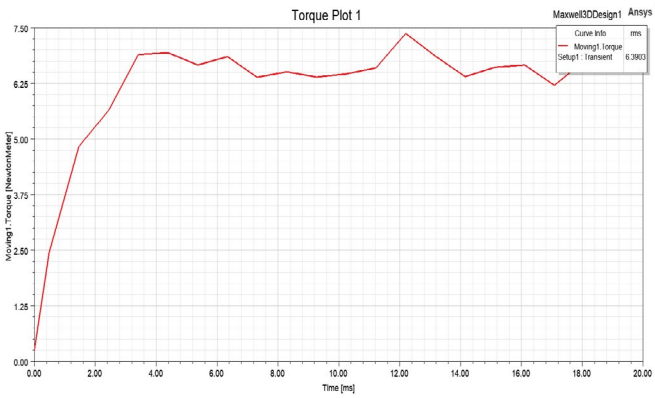

Figure 11. Torque response

Table 2. The BLDC simulation and testing results

Symbol	Parameters	Study	FEM	BLDC-D5BLD 300-12 Test	Unit
P_o	Rated capacity	345	345	300	W
N_{dm}	Rated rotation speed	450	445	400	rpm
T	Rated moment	7.32	6.39	5.8	N.m
$E_{PM} = U$	Induced voltage	4	4.1	4	V
I	Rated current	28	28	21.25	A
L	Iron core length	24.2	24.2	-	mm
u_r	Number of wires in a slot	2	2	-	-
N_s	Number of stator slots	51	51	-	
B_r	Residual magnetism	1.1	1.1	-	T
R_{so}	Stator outer radius	99.5	99.5	-	mm
R_{si}	Inner radius of stator	81.5	81.5	-	mm
R_{ro}	Rotor outer radius	112.5	112,5	-	mm
R_{ri}	Inner radius of stator	99.85	99.85	-	mm
h_{PM}	Magnet thickness	2	2	-	mm
p	Number of pole pairs	23	23	-	-
η	Efficiency	91	91	-	%

From the research results in Figure 9, Figure 10 shows the voltage value and stator current value of the motor according to the design research parameters, from which we see the characteristic curve of the true nature, the features that can be

applied in the working process and control of BLDC motors in the current industrial and civil fields. In Figure 11, we see that the torque response of the motor in the simulation always closely follows the actual working of the BLDC motor in reality. This problem when the motor is working, there always needs to be an increase or decrease in speed, a change in torque, direct control of torque at any time, always coincides with the change in speed, suitable (in a total time of 18ms) of the response, with the voltage, current and torque of the BLDC motor.

In general, when analyzing the results of Figure 8, the magnetic flux density is evenly distributed, the current Figure 9 and voltage Figure 10 form is relatively trapezoidal. Then we see in Figure 9 that the torque response is quite stable and established at T = 6.39 N.m. The author gives detailed results of the research and testing in Table 2.

4. CONCLUSION

This paper has successfully researched and designed a high-performance BLDC motor with great potential for application, especially in the field of industrial and civil machinery manufacturing. The main results show that the motor has achieved outstanding advantages, including: Stable performance and operation and high efficiency, up to 91%. The ability to generate large, stable starting torque (reaching 6.39 N.M in simulation), low maintenance and smooth operation, this issue shows good operating quality, meeting the requirements of new designs. In addition, optimizing materials and production costs: The use of high-performance NdFeB magnets not only improves performance but also helps reduce product costs, opening up opportunities for widespread commercialization. Practical applications: This design is optimized for green means of transport such as electric bicycles, electric vehicles, electric cars, and current industrial and civil machinery. Role of simulation: Application of ANSYS Maxwell software and finite element method (FEM) has demonstrated the reliability of the design.

Future directions: The study has laid a solid foundation for further steps, including design optimization using modern algorithms and motor application research for automatic control fields, especially in electric vehicles. Overall, this study has provided a feasible and efficient BLDC motor design, demonstrating strong application potential in the future, especially in the field of transportation in today's industrial and civil machinery.

REFERENCES

[1] Kerem, A. (2021). Design, implementation and speed estimation of three-phase 2 kW out-runner permanent magnet BLDC motor for ultralight electric vehicles. Electrical Engineering, 103(5): 2547-2559. https://doi.org/10.1007/s00202-021-01279-5

[2] Guguloth, B., Shravani, P., Siva Surya Prakash, T.S. (2024). ANSYS Maxwell simulation for a 2 kW BLDC motor design. In 2024 IEEE International Conference on Intelligent Systems, Smart and Green Technologies (ICISSGT), Visakhapatnam, India, pp. 18-23. https://doi.org/10.1109/ICISSGT58904.2024.00014

[3] Bansal, R., Marwaha, S., Verma, C. (2022). Cogging torque minimization of PMBLDC motor for application in battery electric vehicle. Journal of Electrical Engineering & Technology, 18(3): 1733-1743. https://doi.org/10.1007/s42835-022-01322-w

[4] Hanselman, D.C. (2003). Brushless Permanent Magnet Motor Design. The Writers' Collective.

[5] Ren, K., Chen, H., Sun, H., Wang, Q., Sun, Q., Jin, B. (2023). Design and analysis of a permanent magnet brushless DC motor in an automotive cooling system. World Electric Vehicle Journal, 14(8): 228. https://doi.org/10.3390/wevj14080228

[6] Rauth, S.S., Samanta, B. (2020). Comparative analysis of IM/BLDC/PMSM drives for electric vehicle traction applications using ANN-based FOC. In 2020 IEEE 17th India Council International Conference (INDICON), New Delhi, India, pp. 1-8. https://doi.org/10.1109/INDICON49873.2020.9342237

[7] Wu, Y.C., Lin, B.W. (2012). Computer-aided design of a brushless DC motor with exterior-rotor configuration. Computer-Aided Design and Applications, 9(4): 457-469.

[8] Kumar Potnuru, U. (2020). Design optimization of a permanent magnet brushless DC motor for power density enhancement for a particular application. International Journal of Advanced Trends in Computer Science and Engineering, 9(4): 5748-5755. https://doi.org/10.30534/ijatcse/2020/230942020

[9] Motorola Optoelectronics Device Data. http://bitsavers.informatik.uni-stuttgart.de/components/motorola/_dataBooks/1989_Motorola_Optoelectronics_Device_Data.pdf.

[10] Liu, C., Wang, S., Yang, J. (2024). Thresholding of polarimetric SAR images of coastal zones based on three-component decomposition and likelihood ratio. IEEE Geoscience and Remote Sensing Letters, 21: 1-5. https://doi.org/10.1109/LGRS.2024.3407848

[11] Gamazo-Real, J.C., Martínez-Martínez, V., Gomez-Gil, J. (2022). ANN-based position and speed sensorless estimation for BLDC motors. Measurement, 188: 110602. https://doi.org/10.1016/j.measurement.2021.110602

[12] Ba, D.X., Yeom, H., Kim, J., Bae, J. (2018). Gain-adaptive robust backstepping position control of a BLDC motor system. IEEE/ASME Transactions on Mechatronics, 23(5): 2470-2481. https://doi.org/10.1109/TMECH.2018.2864187

[13] Naseri, F., Farjah, E., Schaltz, E., Lu, K., Tashakor, N. (2021). Predictive control of low-cost three-phase four-switch inverter-fed drives for brushless DC motor applications. IEEE Transactions on Circuits and Systems I: Regular Papers, 68(3): 1308-1318. https://doi.org/10.1109/TCSI.2020.3043468

[14] Patil, M.S., Medhane, R., Dhamal, S.S. (2020). Comparative analysis of various DTC control techniques on BLDC motor for electric vehicle. In 2020 7th International Conference on Smart Structures and Systems (ICSSS), Chennai, India, pp. 1-6. https://doi.org/10.1109/ICSSS49621.2020.9201982

[15] Lakhdara, A., Bahi, T., Izgheche, Y., Henchiri, A. (2025). Improving speed tracking performance of PMSM-driven electric vehicles using a hybrid SMC-MPC approach. Journal Européen des Systèmes Automatisés, 58(9): 1823-1829. https://doi.org/10.18280/jesa.580905

[16] de Almeida, P.M., Valle, R.L., Barbosa, P.G.,

Montagner, V.F., Cuk, V., Ribeiro, P.F. (2021). Robust control of a variable-speed BLDC motor drive. IEEE Journal of Emerging and Selected Topics in Industrial Electronics, 2(1): 32-41. https://doi.org/10.1109/JESTIE.2020.3035055

[17] Wang, L., Zhu, Z.Q., Bin, H., Gong, L.M. (2021). A commutation optimization strategy for high speed brushless DC drives with inaccurate rotor position signals. In 2021 Sixteenth International Conference on Ecological Vehicles and Renewable Energies (EVER), Monte-Carlo, Monaco, pp. 1-9. https://doi.org/10.1109/EVER52347.2021.9456659

[18] Chokkalingam, B., Yusuff, A., Tariq, M., Bhekisiph, T. (2019). Torque-ripple mitigation for BLDC using integrated converter connected three-level T type NPC-MLI. In 2019 International Conference on Electrical, Electronics and Computer Engineering (UPCON), Aligarh, India, pp. 1-6. https://doi.org/10.1109/UPCON47278.2019.8980096

[19] Duraisamy, K., Shanmugam, B., MohanRam, N., Chinniah, P., Mohideen, J.M., Ramalingam, A. (2025). A quick and effective current-based approach for BLDC motor interturn fault identification using artificial neural network. Journal Européen des Systèmes Automatisés, 58(6): 1237-1244. https://doi.org/10.18280/jesa.580613

[20] Lee, S.T., Hur, J. (2017). Detection technique for stator inter-turn faults in BLDC motors based on third-harmonic components of line currents. IEEE Transactions on Industry Applications, 53(1): 143-150. https://doi.org/10.1109/TIA.2016.2614633

[21] Shifat, T.A., Hur, J.W. (2021). ANN assisted multi sensor information fusion for BLDC motor fault diagnosis. IEEE Access, 9: 9429-9441. https://doi.org/10.1109/ACCESS.2021.3050243

[22] Singh, A., Yadav, S., Sarangi, S., De, S., Singh, A.K., Singh, R.K. (2025). Optimizing BLDC motor performance: A study of PID, artificial neural network and fuzzy logic controllers. In 2025 International Conference on Innovation in Computing and Engineering (ICE), Greater Noida, India, pp. 1-6. https://doi.org/10.1109/ICE63309.2025.10984074

[23] Sundaram, M., Anand, M., Chelladurai, J., Varunraj, P., Joshua Smith, S., Sharma, S., El Haj Assad, M., Alayi, R. (2022). Design and FEM analysis of high-torque power density permanent magnet synchronous motor (PMSM) for two-wheeler e-vehicle applications. International Transactions on Electrical Energy Systems, 2022: 1-14. https://doi.org/10.1155/2022/1217250

[24] Boldea, I., Nasar, S.A. (2010). The Induction Machine Handbook. CRC Press.

[25] Lukman, G.F., Son, D.H., Lee, D.H., Ahn, J.W. (2017). Design of in-wheel type switched reluctance motor for electric vehicle traction and wireless charging. The Korean Institute of Electrical Engineers, 66(12): 1866-1872. https://doi.org/10.5370/KIEE.2017.66.12.1866

NOMENCLATURE

T	Rated torque, Nm
ϑ_m	Mechanical angular velocity
N_s	Number of stator slots
f_e	Basic electrical frequency

Greek symbols

α	Step coefficient
θ	Extreme step angle
τ_p	Stator pole step
Φ	The air gap flux
ω	Angular speed

Subscripts

ref	Reference
shaft	The shaft power
output	The transmitted power calculated